

NIBS2022 (3-7 Oct. 2022), oral presentation, Tuesday 4 October 2022, Padova, Italy

# Fluid models of radiofrequency coupling and plasma density for ion sources as NIO1



Marco Cavenago<sup>1</sup>



<sup>1</sup>INFN-Laboratori Nazionali di Legnaro (LNL), v.le dell'Università 2, I-35020, Legnaro (PD) Italy

- 1) Introduction: inductive plasma heating***
- 2) The rf conductivity in bounded plasmas (and the skin depth)***
- 3) Non-magnetized plasmas***
- 4) Magnetized plasmas and model***
- 5) Simulations workflow, and results for magnetized plasma***
- 6) Conclusions***

# 1) Introduction

Ionized gases, also known as plasmas, need a continuous influx of energy, also known as heating, to maintain ionization. Heating methods: (a) microwave and (b) radiofrequency (not dissimilar from microwave food cooking); (c) arc. Microwaves/rf are often preferred in plasmas for ion production [ ...]

the plasma angular frequency

$$\omega_p = \sqrt{n_e e^2 / (m_e \epsilon_0)}$$

depends on electron density  $n_e$

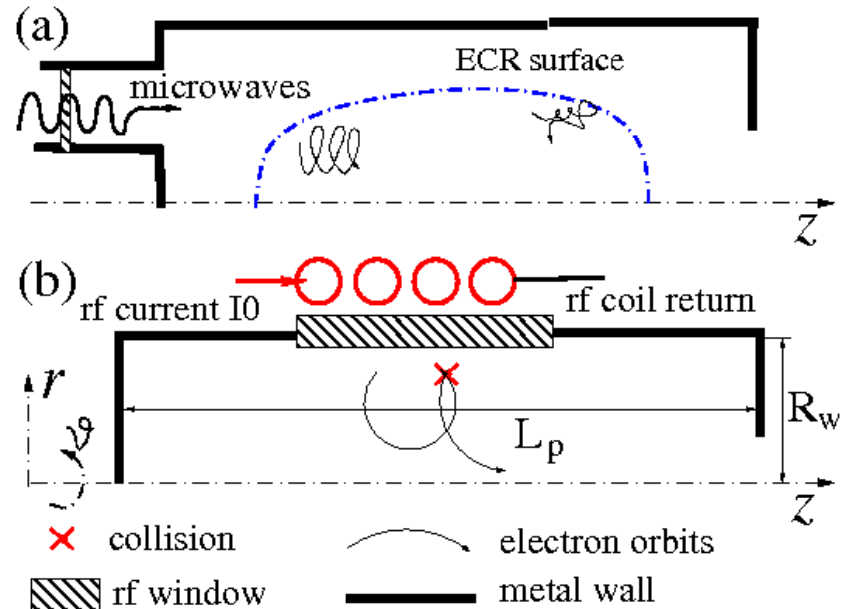
When  $n_e$  equals to the cutoff density  $n_c$

$$n_c = m_e \epsilon_0 \omega^2 / e^2$$

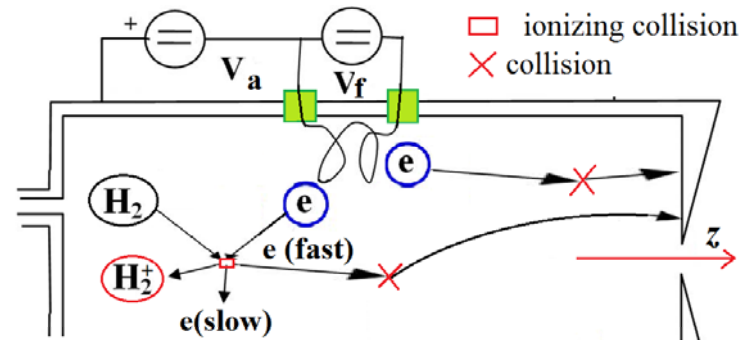
where  $\omega$  is the angular microwave frequency, we have

$$\omega = \omega_p$$

Typically  $n_e = 10^{18} \text{ m}^{-3}$  in ion source center, so microwave source (ECRIS [4]) are below cut off density and radiofrequency plasma (b) have density over the cutoff



(a) ECRIS (Electron Cyclotron Resonance Ion Source [4]);  
 (b) Inductively Coupled Plasma (ICP).



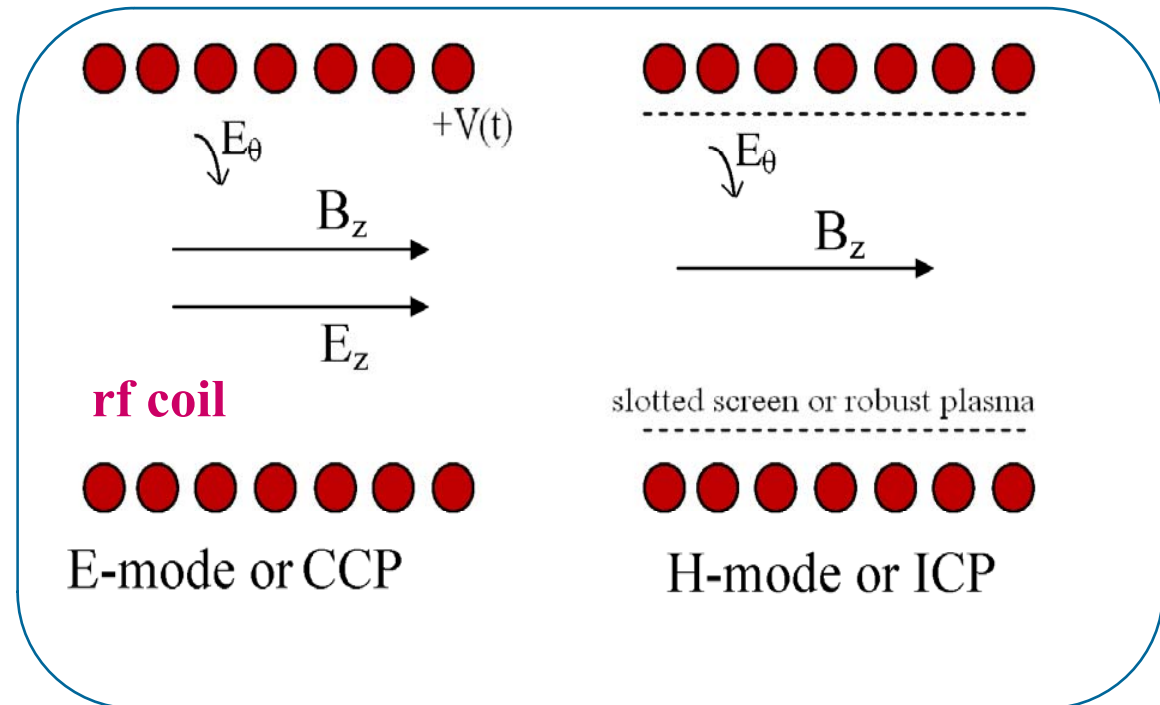
(c) arc: a known current of e- fast ionizes (red dots) gas, giving  $\text{H}_2^+$  and (cold) e

## The plasma can couple to rf coil in two modes

1) **Capacitive Coupled Plasma (E-Mode : very low electron density, the axial electric field  $E_z$  [13] directly accelerates them, and deconfines them (that,  $E_z$  pushes them out of the plasma))**

2) **Inductive Coupled Plasma (H-mode, dense plasma); axial electric field  $E_z$  is suppressed (by a slotted screen or by plasma polarization); the weaker  $E_\theta$  accelerates electrons in multisteps, by stochastic or collision phase mixing, and electron energy distribution is broad (similar to a Maxwellian one).**

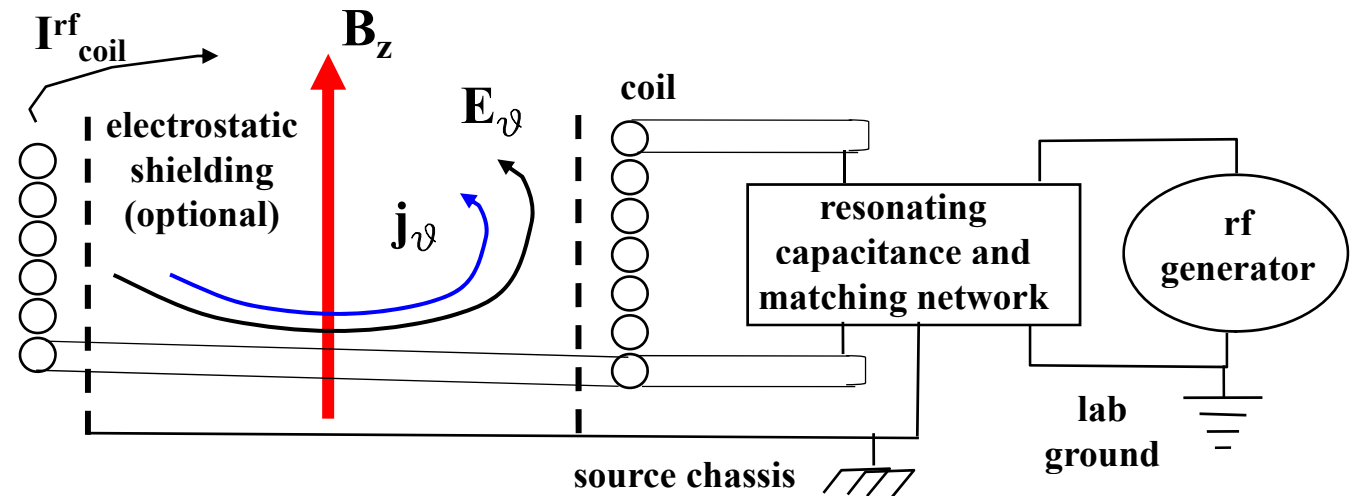
We restrict to this coupling.



## 2) RADIOFREQUENCY (rf) HEATING

a) The simpler model: assuming that plasma behaves as the secondary of a transformer; this model may overestimate efficiencies

There are rf losses in the coil and the metal wall of the vacuum chamber, and in the Faraday shield when used



b) A next simpler model

Assuming conductivity  $\sigma$  is known in plasmas (see later), rf heating is a typical 'lossy dielectric problem' (analogy: cooking; rf ovens for ion sources; cold crucibles )

Plasma (or a screen) shields electric potential, so that only azimuthal part of vector potential remains:

$$\mathbf{A} \cong \Re \hat{\vartheta} A_{\vartheta}(r, z) e^{i\omega t} \quad \phi \cong 0 \quad \Re \text{ (real part of)}$$

is usually understood

$$\text{Maxwell} \Rightarrow r A_{\vartheta,zz} + (r A_{\vartheta,r})_{,r} + r Q A_{\vartheta} = \mu_0 \sigma U_k \quad (2a)$$

where  $U_k$  is applied voltage/radians, a comma means 'partial differentiation' and  $Q$  depends on material

$$Q = -r^{-2} - i\mu_0 \omega \sigma + \epsilon_r (\omega/c)^2 \quad (2b)$$

## 2.2) The conductivity in plasma (mainly due to electrons)

In plasma, rf field strength is not uniform (typically it is decaying, that is the skin effect), and rf includes both magnetic and electric field so electron motion is very complicated, as easily seen in one-particle simulations, also for weak plasma (electron density  $n_e$  to zero)

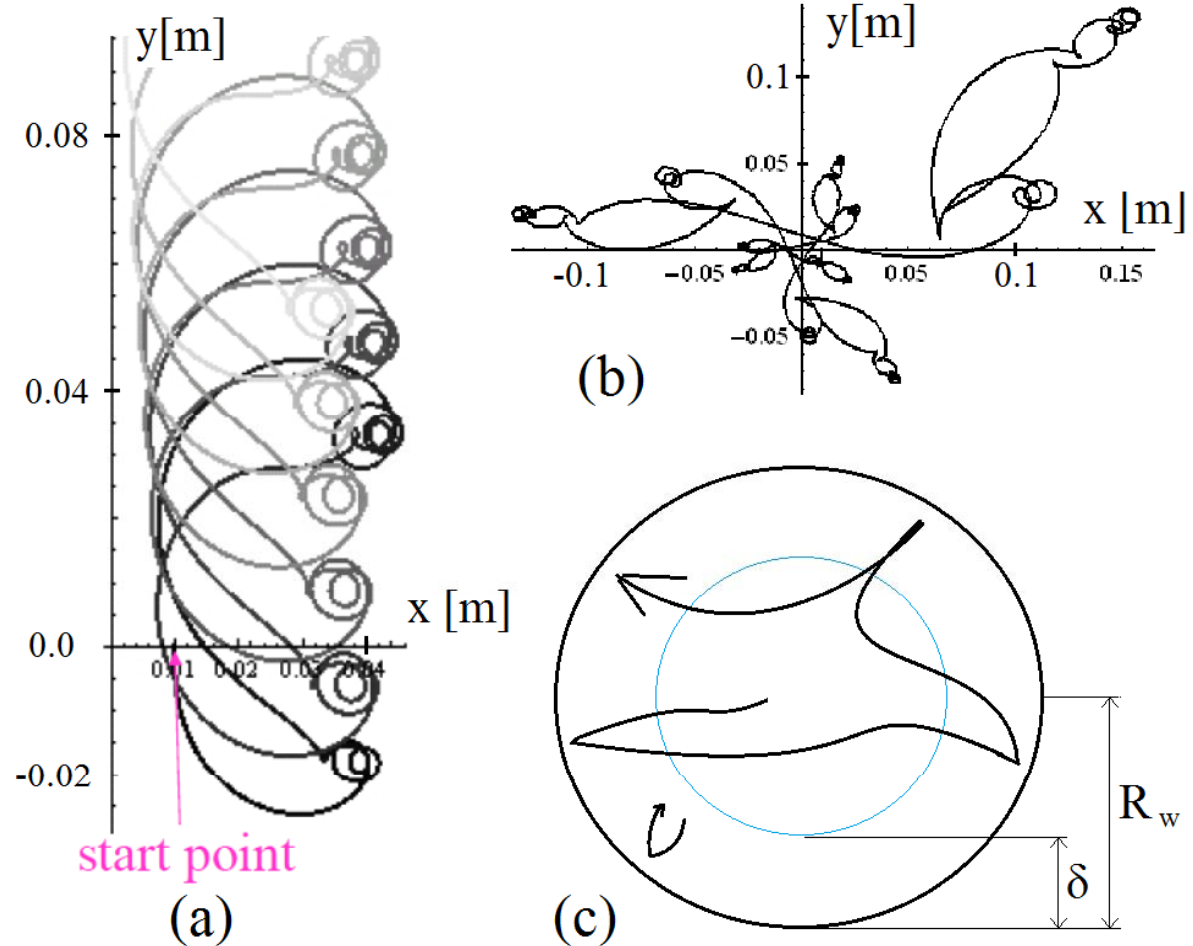


**Figure:** samples of electron orbits in rf fields in  
 (a) weak plasma, uniform  $B_z$  and  $E_r$   
 (b) weak plasma, uniform  $B_z$  and  $E_\theta \propto r$   
 (c) strong plasma, ie skin depth  $\delta$  smaller then radius  $R_w$

### 2.3) the local conductivity $\sigma$ model and the skin depth

Strictly speaking conductivity is nonlocal operator (defined by a functional derivative)

$$\sigma = \delta \mathbf{j} / \delta \mathbf{E}$$

A local expression including only gas collision friction or ‘collision equivalenced’ effect is  $\sigma = n_e e^2 / (v_c + i\omega)$  with  $v_c = v_m + v_s$

$v_m$  collision frequency due to real collision with gas or ions

$v_s$  stochastic term to fit anything else (see section 2.4), like collisions with walls or oscillation larger than skin depth

The material function  $Q$  is then simply

$$Q = \epsilon_r \frac{\omega^2}{c^2} - \frac{1}{r^2} - \frac{\omega_p^2}{c^2} \frac{i\omega}{v_c + i\omega}$$

In induction plasma  $\omega_p \gg \omega, v_c$  skin depth  $\delta$  approximates as

$$\frac{\delta}{c} \simeq \frac{\sqrt{2(1 + \gamma^2)}}{\sqrt{1 + \sqrt{1 + \gamma^2}}} \frac{1}{\omega_s} \quad \gamma = v_c / \omega \quad \omega_s^2 = \omega_p^2 - \omega^2$$

### 3) Non-magnetized plasma: formulas for effective collision frequency

Let us recall that, in some simple case [6] as electron bouncing from a plasma/wall sheath, power absorption can be calculated from kinetic and nonlocal model.

$$\frac{P_w}{|E_w|^2} = n_e^w \frac{e^2 \delta^2}{m_e v_{th}} I_1(\alpha) \quad , \quad \alpha = \frac{4\omega^2 \delta^2}{\pi v_{th}^2}$$

with thermal velocity  $v_{th} = (8T_e/\pi m_e)^{1/2}$

$$I_1(\alpha) = [(1 + \alpha)e^\alpha \Gamma(0, \alpha) - 1]/\pi$$

[The time electron spend inside rf skin layer is  $\tau = 2 \delta/v_{th}$ , so  $\omega\tau$  is a dimensionless parameter, as well  $\alpha$  is ]

The effective coll. frequency is defined such as to obtain the same power absorption which gives

$$\frac{\nu}{1 + \nu^2} \cong 2\sqrt{\pi\alpha} I_1(\alpha)$$

This has two solution for  $\nu$ , shown  $\nu^+$  or  $\nu^-$  in the figure. Also compare [Jain,2018]

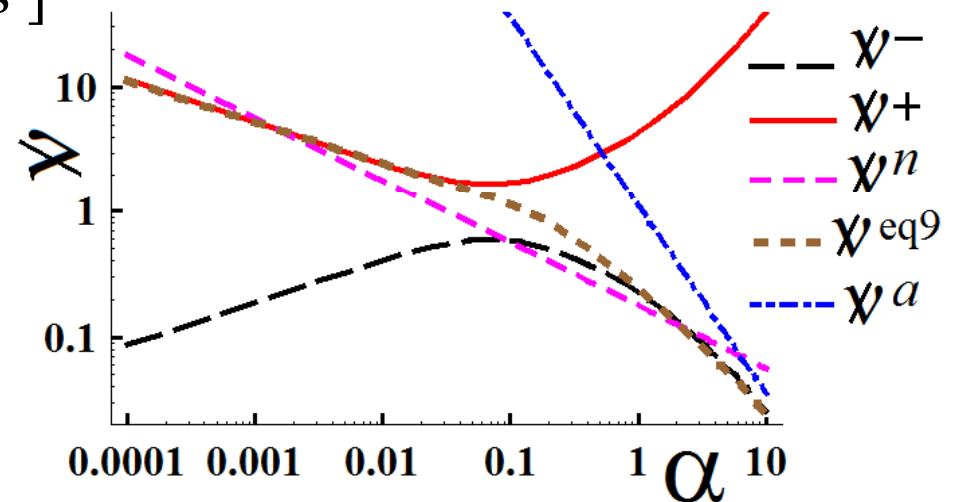


Figure: Plots of  $\nu_c/\omega$  vs  $\alpha$ , from eqs. (8) or (9) in [Cavenago, GASS 2020 (virtual, IEEEExplore)]

## 4) Magnetized plasmas and plasma model

We have

$$B_z = B_f \sin(\omega t) + B_s, \quad E_\theta = \frac{1}{2} \omega r B_f \cos(\omega t)$$

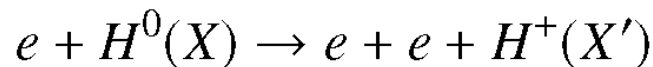
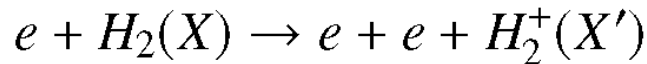
with static magnetic fields  $B_s$ , which gives the well known cyclotron frequency  $\Omega_s = e B_s / m_e$ , and rf magnetic field with amplitude  $B_f$ , and similarly  $\Omega_f = e B_f / m_e$ . We can combined both as

$$\Omega_t^2 = \frac{1}{2} \Omega_f^2 + \Omega_s^2$$

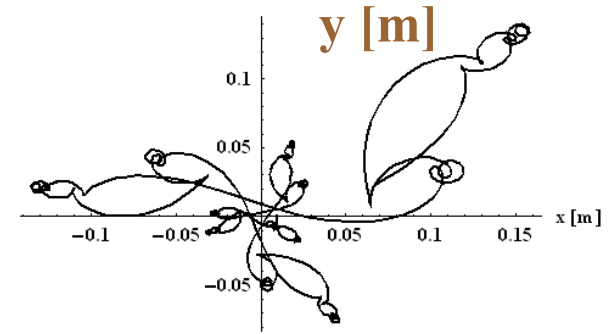
**Generalizing ref [Tuszewski, 1997 Phys. Plasmas] formula, for  $\omega \ll \nu_c < \Omega_t$  the conductivity is about**

$$\langle \sigma \rangle = \frac{n_e e^2}{m_e \sqrt{\nu_c^2 + \Omega_t^2}} \left( 1 - \frac{i \omega \nu_c}{\nu_c^2 + \Omega_t^2} + O(\nu_c^2) \right)$$

**2D MODEL** The static magnetic field is azimuth averaged as  $B^s = \left[ \int d\vartheta |\mathbf{B}^s|^2 / (2\pi) \right]^{1/2}$



**TOTAL IONIZATION RATE**  $n_g n_e K_{iz}(T_e) = n_{iz}$



**Motion of e- with  $B_f = 5$  G and  $B_s = -2$  G**

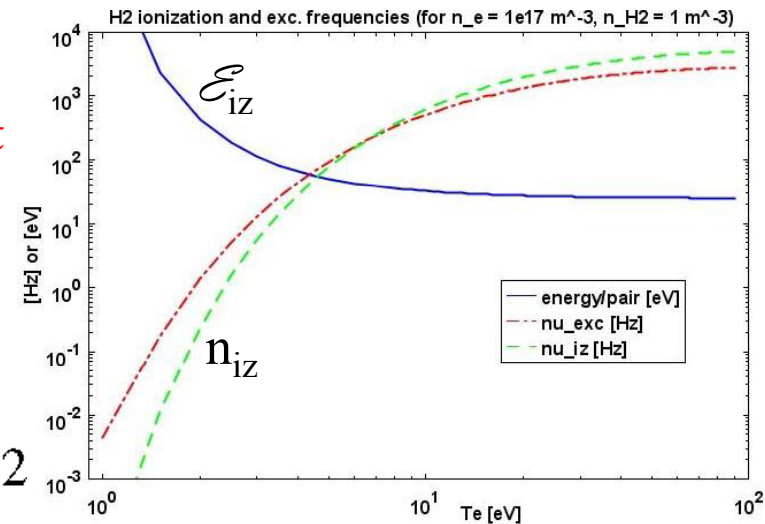


Figure:  $\mathcal{E}_c$ , the energy lost per pair (e ion+) produced vs the plasma electron temperature  $T_e$ ; note its peak for  $T_e < 3$  eV. Reason is that excitation rate is there much greater than ionization rate, as shown



Plasma heat diffusion balances with electromagnetic heat  $P_h$  and energy loss in ionization

$$-\nabla(K_e \nabla T_e) = P_h - n_e n_g K_{iz} \mathcal{E}_{iz}$$

$$P_h = \frac{1}{2} \Re(j_{\vartheta}^* E_{\vartheta})$$

$$u_B = \sqrt{T_e / M_i}$$

$$K_e = \frac{3n_e T_e \nu_m}{2m(\nu_m^2 + \Omega_s^2 + \Omega_f^2)^{1/2}}$$

where  $K_e$  is thermal conductivity,  $u_B$  the Bohm speed,  $K_{iz}(T_e)$  is the ionization constant (see graph for  $n_{iz}$ ) and  $\mathcal{E}_{iz}$  is the energy loss per ionization pair (see graph)

Ions accelerated by sheaths before they hit wall where their energy is wasted. Since typical sheath are localized and requires a thin mesh for PDE solution, we exclude them from PDE solution domain, including known sheath effect in boundary conditions:

$$-K_e \mathbf{n} \cdot \nabla T_e = u_B n_e \phi_d$$

(with  $\mathbf{n}$  the outward normal vector), that is the heat flow at wall equals the energy lost by ions

$$\phi_d = \frac{1}{2} T_e \ln[M / 2\pi m]$$

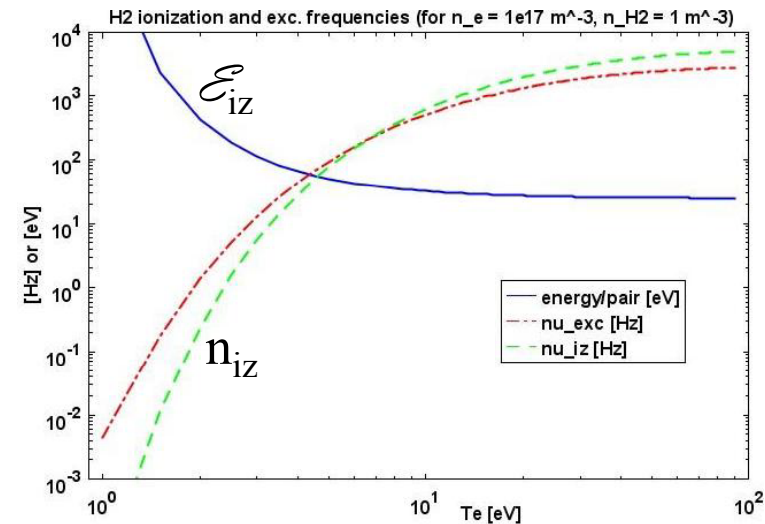


Figure:  $\mathcal{E}_c$ , the energy lost per pair (e ion+) produced vs the plasma electron temperature  $T_e$ ; note its peak for  $T_e < 3$  eV. Reason is that excitation rate is there much greater than ionization rate, as shown

**MODEL** We require quasi neutrality  $n_e + n_H^- = n_i$

that is  $n_e = n_i$  (positive ion) almost everywhere (since we get H- only near extraction) and that flow of electrons  $\Gamma_e$  originates from ionization rate  $n_{iz}$  as the flow of ions  $\Gamma_i$  does

$$\text{div } \Gamma_i = \text{div } \Gamma_e = n_g n_e K_{iz}(T_e) = n_{iz}$$

**DIFFUSION** The slower charges (ions typically) drag the opposite charges, so

$$\Gamma_i = -D_a \text{grad} \left( n_e + s_p \frac{B_f^2}{4\mu_0 T_e} \right) \quad \text{or simply} \quad \Gamma_i = -D_a \text{grad } n_e$$

neglecting the ponderomotive  $B^f$  effects ( $s_p=0$ ), with  $D_a$  the ambipolar diffusion coefficient. Let the ambipolar diffusion velocity  $v_a$  and the ion thermal speed  $v_{th}^i$  be

$$\mathbf{v}_a = \Gamma_i / n_e \quad v_{th}^i = \sqrt{T_i / M_i}$$

when  $v_a$  much lower  $v_{th}^i$ ;  $D_a \cong T_e / M_i v_i$   
 otherwise,  $D_a$  is smoothly reduced so that  $v_a \leq v_{th}^i$

**BOUNDARIES** Some secondary electron emission (SEE) from wall may help plasma (and in ECRIS source wall coating effect was well known; Drentje, 2003, Bentounes, 2018); so we call  $s_{ee}$  the fraction of e/ions (re)emitted from walls

$$-D_a \mathbf{n} \cdot \text{grad } n_e \equiv \mathbf{n} \cdot \Gamma_i = n_e (1 - s_{ee}) \sqrt{T_e / M_i}$$

## 5) Solution and results: 5.1 Work flow of a typical multiphysics simulation

There are two good reasons for iterative solving of previous model:

- 1) Some variable (as  $n_e$  or  $T_e$ ) are real valued, some are complex (magnetic potential phasor), so  $n_e$  and  $T_e$  must be kept real against rounding error effects
- 2) The problem is nonlinear (it may have many solutions in principle), so the user has to give an adequate initial guess, which is easier for real variables alone
- 3) PDE are singular at  $n_e = 0$  and  $T_e = 0$ , so we impose  $n_e > 0$  and  $T_e > 0$

As practical fact, computer RAM is limited (not a TB yet): so in our code solution is also performed in 2D with preliminary averaging of the static magnetic field (which has a 3D structure, with strong multipoles).

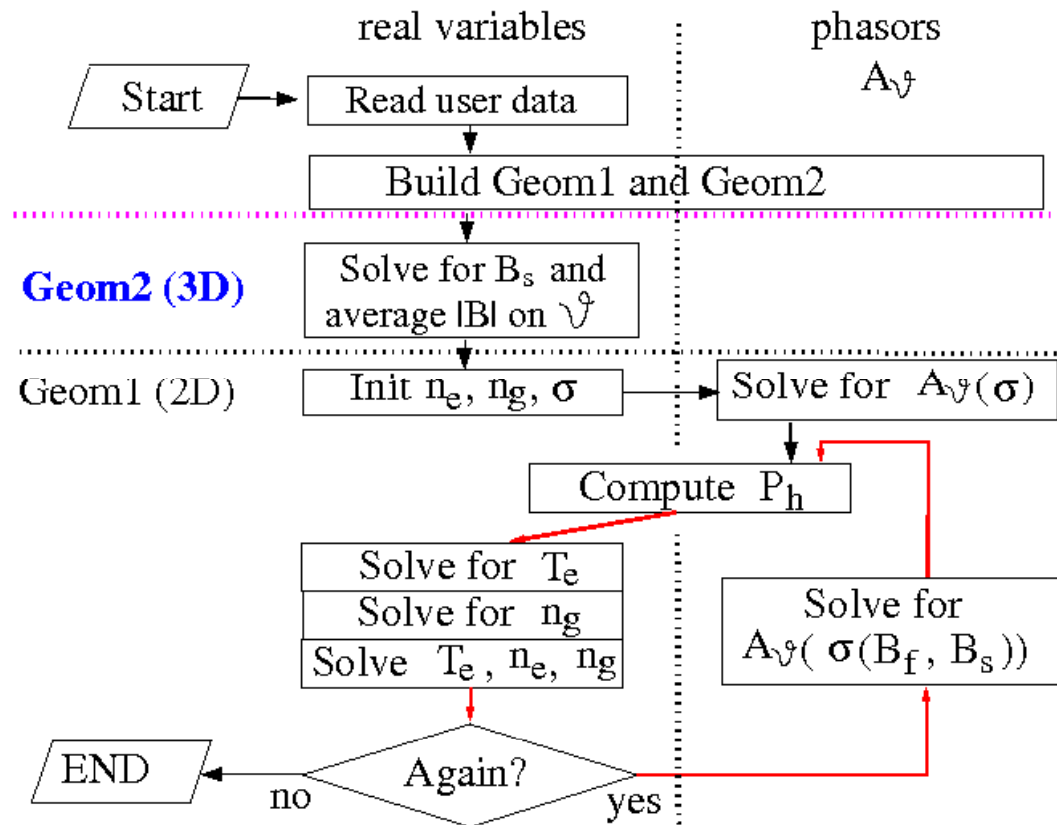


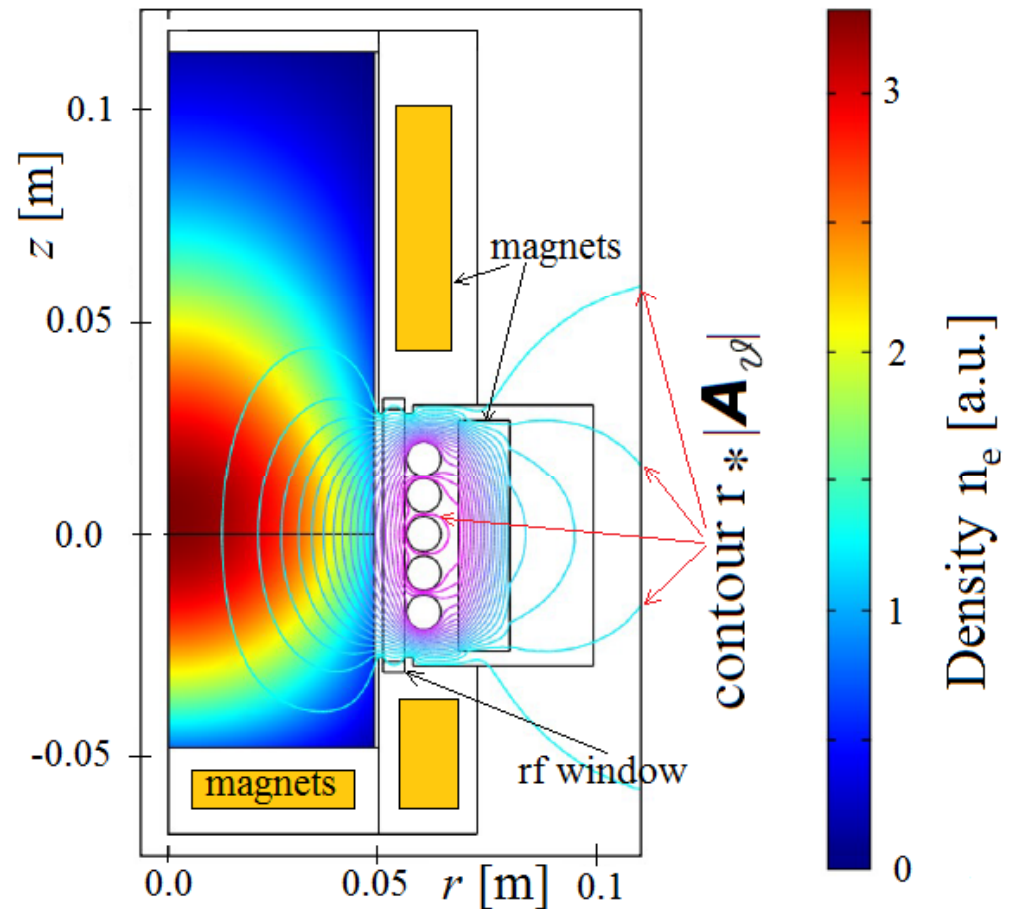
**Figure 5. Major steps of numerical simulations.**

## 5.2) Results; $s_{ee}=0$ case

Beware: Any correct model of ionization and rf absorption in plasma typically includes a possible instability: the more electron are produced the more rf power can be adsorbed which gives even more electrons, provided gas density  $n_g$  and coil current is kept constant. Stabilization is more easily inbuilt in the model by adjusting gas density so to have a reasonable plasma density at given point (set by experience or as experimental input data)

Once model has converged, the density typically peaks on source axis, where plasma confinement is better (so more plasma accumulates)

Similarly the induction rf filter peaks on the rf coil; it is possible to define pseudo flux lines of rf magnetic field, as the contour level of  $r |A_{\theta}|$ ; the absolute value takes care of phasor rf field and in static limit, gives the usual flux line



Plasma density  $n_e$  and 'pseudo-flux-lines' of rf magnetic field (that is, level curve of  $r |A_{\theta}|$ ). Note the old NIO1 design with only 5 turn coils

## 5.2.1) NIO1 with 7 turn coil as built

Static magnetic field is provided in NIO1 by 3 terms: a strong rear multipole; a significant field near PG, due to the fringe field of accelerator electrodes; a filter field, with a bell shaped z-profile centered in the front region (filter field strength  $B_{fa}$  is adjustable)

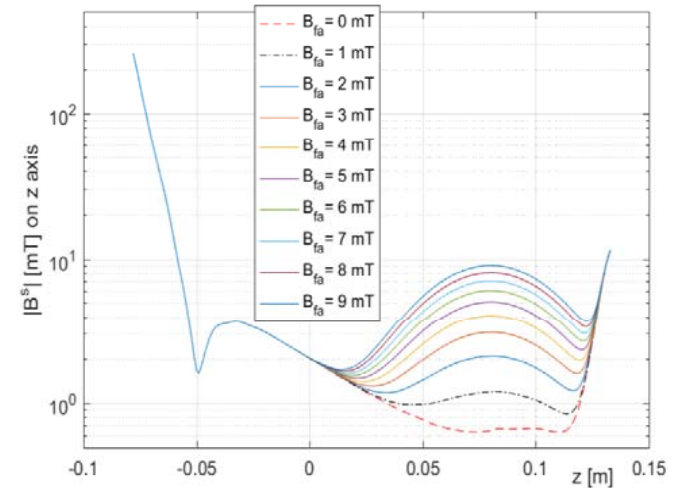
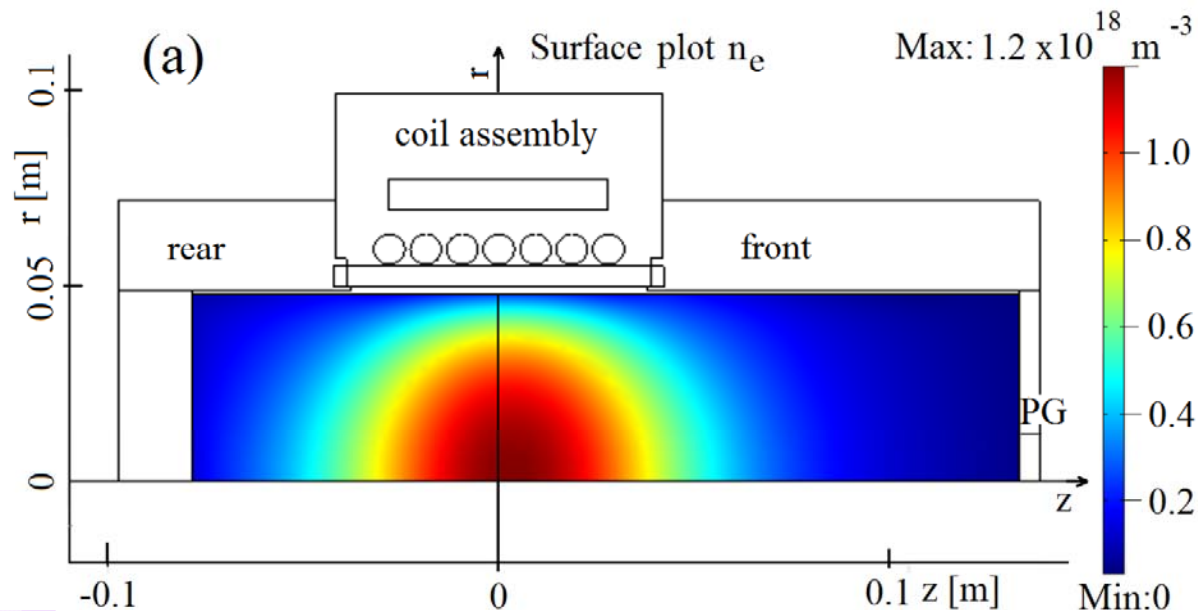
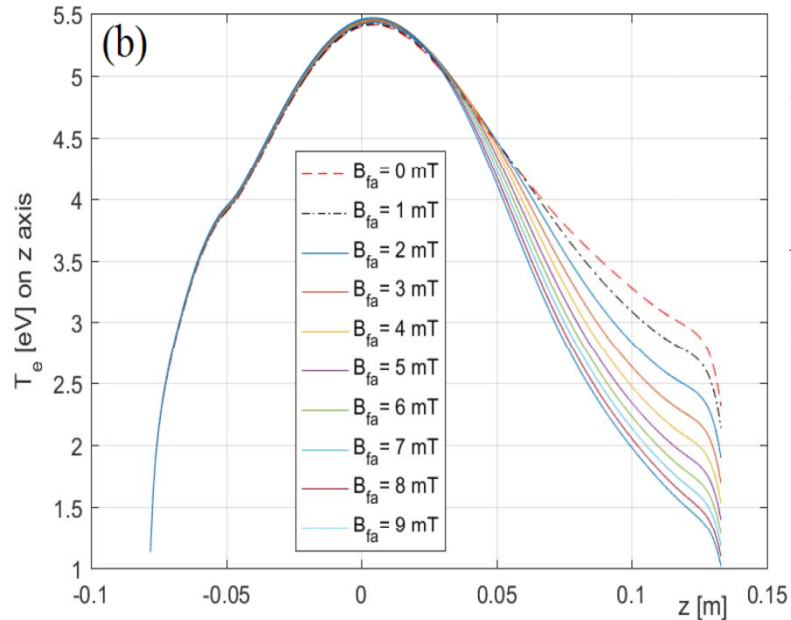


Figure 6. Total field strength, for filter strength from  $B_{fa} = 0$  to 9 mT

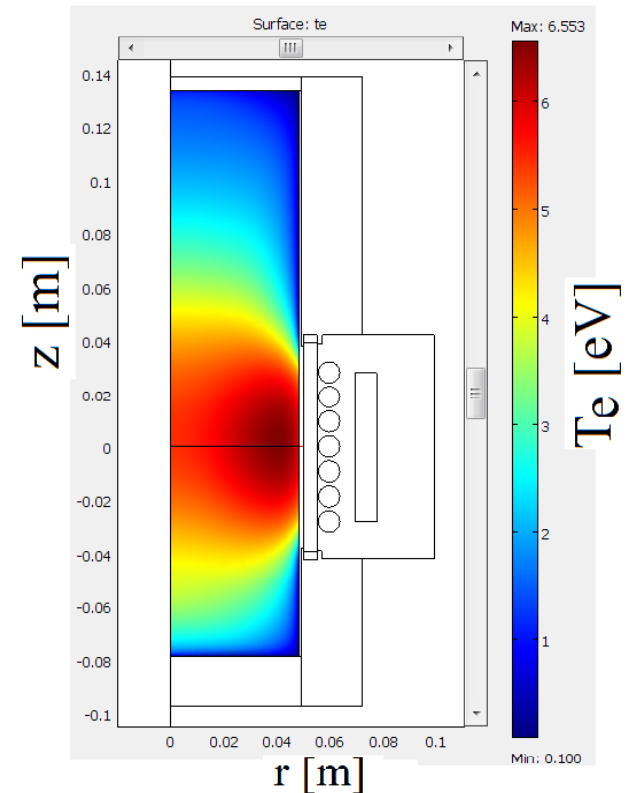
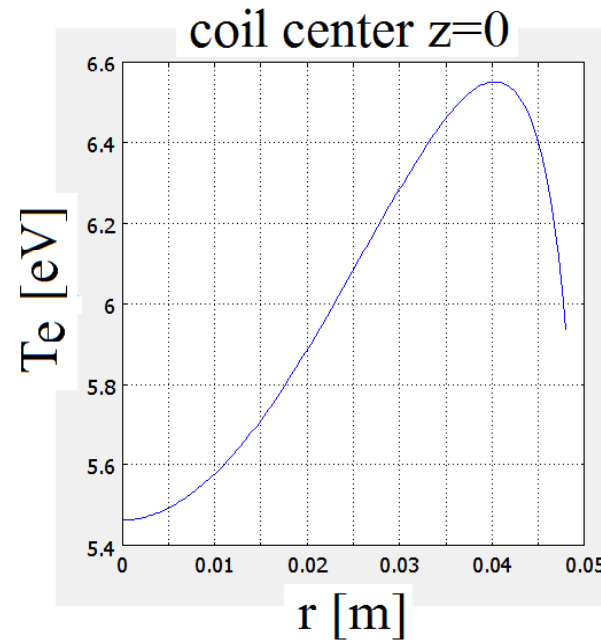


(a) Result for density  $n_e$ , with  $B_{fa} = 8$  mT with rf power 1300 W and gas pressure about 0.75 Pa



Result for  $T_e$  on z-axis, with rf power 1300 W and gas pressure about 0.75 Pa, for ranging  $B_{fa}=0 \dots 9$  mT .

Note that  $T_e < 2\text{eV}$  at extraction region  $z > 0.11$  m requires  $B_{fa} > 7$  mT, as usually set in the experiments



Result for  $T_e$ , with  $B_{fa}=8$  mT with rf power 1300 W and gas pressure about 0.75 Pa

**M. Cavenago "Radiofrequency coupling and plasma density", NIBS'22, Padova, Italy**

### 5.3) Results; $s_{ee} > 0$ case

Here we show how plasma equilibrium depend from assumed see, for a sensitivity study (to be later rapidly compared with experiments). In principle, see can be any function of boundaries, but we restrict to three zones and parameters. On metal walls,  $s_{ee}=s_0$  (with value scanned  $<0.4$ ); on dielectric walls, we add a quantity  $s_1 < 0.4$ , so that  $s_{ee}=s_0+s_1$ . In both zones

$$s_{ee} = s_0 + s_1 \Theta_s(z_w - |z|, w)$$

where  $z_w=38$  mm from NIO1 geometry,  $\Theta_s$  is a smoothed Heaviside function. Optionally, an extraction effect can be added assuming  $s_{ee}=0$  at extraction, for  $r < r_h$  (11.4 mm for equal area)

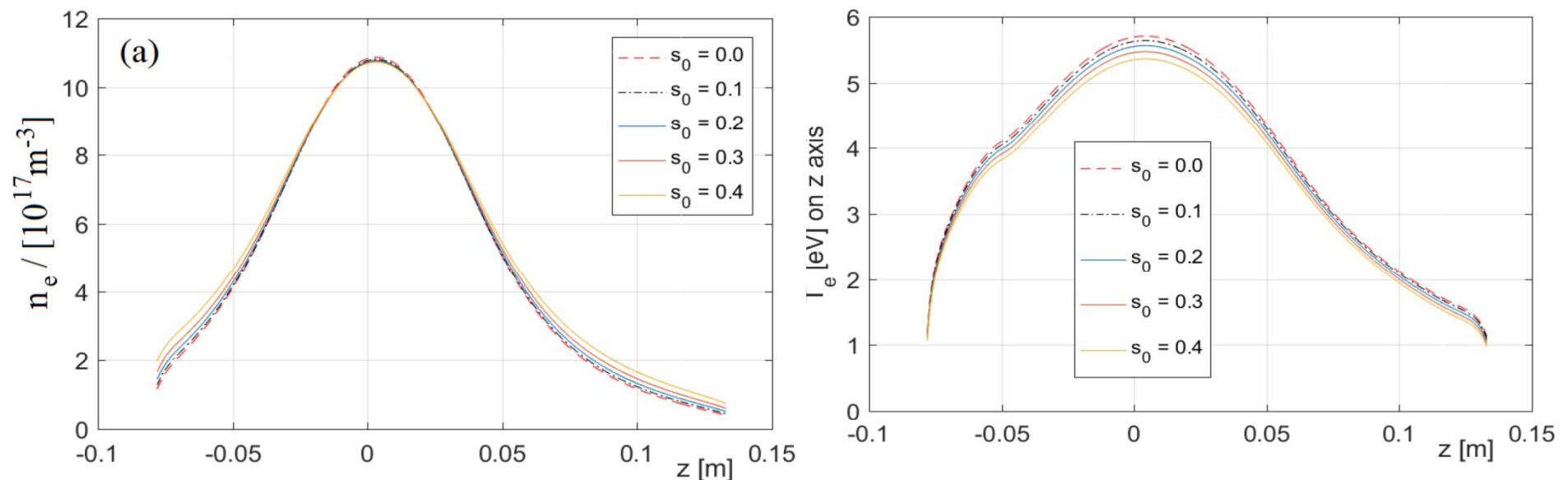
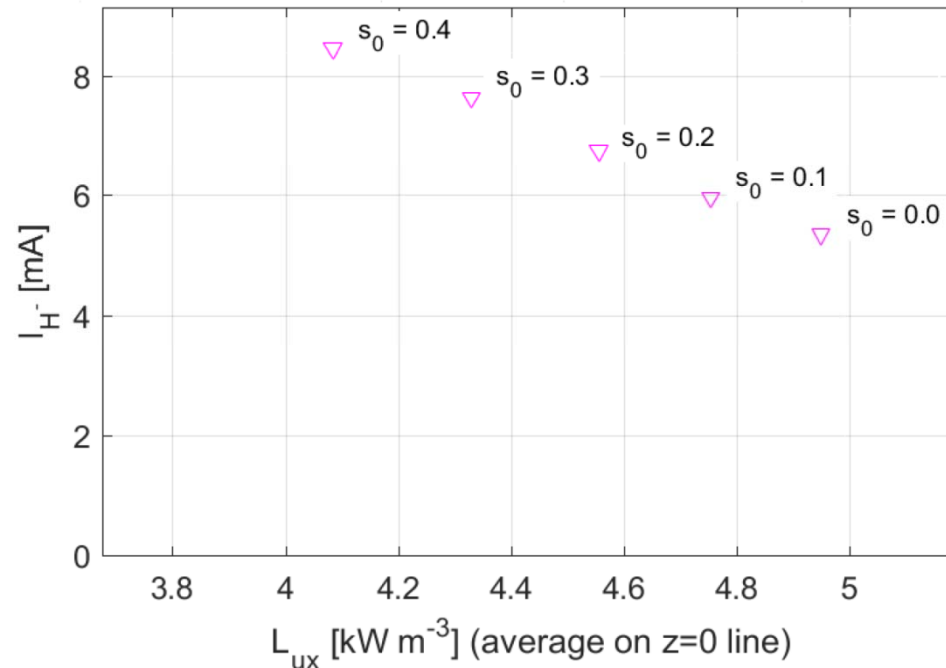


**Figure 8.** a) axial density  $n_e|_{r=0}$  vs  $z$ , for increasing wall coefficient  $s_0$  in eq. 6.10, at fixed  $s_1 = 0.2$ ,  $B_{fa} = 8$  mT,  $p_s \cong 0.7$  Pa and  $P_s = 1300$  W; (b) axial temperature  $T_e$  for the same cases.

Note the differences in central  $T_e$  and in extraction  $n_e$

## continue 5.3) Results; $s_{ee} > 0$ case

Finally, from known profiles of  $n_e$  and  $T_e$ , and atomic data [Johnson, 1973] a global plasma luminosity for any line of sight (in particular, for the axial line of sight of NIO1) can be calculated, and is very sensitive to central  $T_e$ . Also the extraction current in Cs-free regimes can be guessed with comparison to previous works [Pagano, 2007, Mossbach 2005) for the  $n_{H^-}/n_e$  relation. We have  $I_{H^-}$  growth with  $n_e$  and  $1/T_e$  as expected. More work to calculate  $I_{H^-}$  directly from  $n_e$  and  $T_e$  profile is in progress.



**For previous slide cases, estimated plasma light emission  $L_{ux}$  and ion current  $I_{H^-}$ .**

In conclusion, the model is able to predict an anti-correlation of  $L_{ux}$  and  $I_{H^-}$  (at constant source power and pressures) always observed in NIO1. In particular the gas conditioning experiment (in Cs-free regime until 2019) show that wall can be conditioned, with results as in the above figure range.



## 6) CONCLUSION

Induction heating involve both particle and EM field modeling. While a calculation of each electron trajectory is clearly too long especially for ion source design, a vast literature has developed useful approximation to this problem, introducing the so called stochastic heating, with several formulas here reviewed. Induction heating of plasma so reduces to typical nonlinear problem of partial differential equation (PDE), with gas ionization rate and rf power absorption in positive feedback. Stability is obtained (both in the experiment and in the modeling) by the limited amount of rf power and gas available. Relation between physical boundary condition and possible wall status (similar to known effect in ECRIS) was introduced and parameterized by a  $s_{ee}$  coefficient. The simple model solution well reproduce observed trends for gas density, equivalent plasma resistance and plasma luminosity. Most of all, solution are sensitive to  $s_{ee}$  in a way consistent with some experimental evidence from NIO1.

### Acknowledgements

Work supported by experiment Ion2neutral (group 5 of INFN, Istituto Nazionale di Fisica Nucleare) and project INFN-E (Energy applications)

# THANK YOU FOR ATTENTION

(see bibliography next slides)

## References

- [1] M. A. Lieberman and V. A. Godyak, "From Fermi Acceleration to Collisionless Discharge Heating," *IEEE Trans. Pla. Sci.*, 26, 1998, pp. 955–986, doi:10.1109/27.700878.
- [2] M. A. Lieberman and A. J. Lichtenberg, "Principles of Plasma Discharges and Materials Processing," New York, Wiley, 2005 (2nd ed.), doi:10.1002/0471724254.
- [3] I. D. Kaganovich, V. I. Kolobov, and L. D. Tsendin, "Stochastic electron heating in bounded radio-frequency plasmas" *Appl. Phys. Lett.*, 69, 1996, pp. 3818–3820, doi:10.1063/1.117115.
- [4] G. Torrioni, D. Mascali, A. Galatà, et al., "Plasma heating and innovative microwave launching in ECRIS: models and experiments," *J Instrum*, 14, 2019, C01004, and references therewithin, doi:10.1088/1748-0221/14/01/C01004.
- [5] M. Cavenago and C. T. Iatrou, "Studies on microwave coupling into the electron cyclotron resonance ion source Alice," *Rev. Sci. Instrum.*, 65, 1994, pp 1122– 1124, doi:10.1063/1.1145084.
- [6] V. Vahedi, M. A. Lieberman, G. DiPeso, T. D. Rognlien, and D. Hewett, "Analytic model of power deposition in inductively coupled plasma sources," *J. Appl. Phys.*, 78, 1995, pp. 1446–1458, doi:10.1063/1.360723.
- [7] M. Cazzador, M. Cavenago, G. Serianni, and P. Veltri, "Semi-analytical modeling of the NIO1 source," *AIP Conf. Proc.*, 1655, 2015, 020014, doi:10.1063/1.4916423.
- [8] M. Tuszewski, "Inductive electron heating revisited," *Phys. Plasmas*, 4, 1997, pp. 1922–1928, doi:10.1063/1.872335.
- [9] P. Jain, M. Recchia, M. Cavenago, U. Fantz, E. Gaio, W. Kraus, A. Maistrello and P. Veltri, "Evaluation of power transfer efficiency for a high power inductively coupled radiofrequency hydrogen ion source," *Plasma Phys. Control. Fusion*, 60, 2018, 045007, doi:10.1088/1361-6587/aaab19.
- [10] D. Rauner, S. Briefi and U. Fantz, "RF power transfer efficiency of inductively coupled low pressure H2 and D2 discharges," *Plasma Sources Sci. Technol.*, 26, 2017, 095004, doi:10.1088/1361-6595/aa8685.
- [11] F. F. Chen, "Nonlinear Effects and Anomalous Transport in RF Plasmas," *IEEE Trans. Pla. Sci.*, 34, 2006, pp. 718–727, doi:10.1109/TPS.2006.874851.
- [12] M. Cavenago and S. Petrenko, "Models of radiofrequency coupling for negative ion sources," *Rev. Sci. Instrum.*, 83, 2012, 02B503, doi:10.1063/1.3670601.
- [13] K. Henjes. "Electric and magnetic fields in solenoidal coils from statics to MHz Frequencies", *J. Appl. Phys.*, 79 (1996) 21-29.
- [14] S. Lee, Y. Lee and Yu I., "Electric Field in Solenoids", *Jpn. J. Appl. Phys.*, 44 (2005) 5244-5248

## More references

- [1] R. S. Hemsworth and D. Boilson, AIP Conf. Proc. 1869 (2017) 060001.
- [2] H. Zohm, C. Angioni, E. Fable, et al., Nucl. Fusion, 53 (2013) 073019 [3] J. Peters, Rev. Sci. Instrum. 79 (2008) 02A515.
- [4] M. P. Stockli, B. X. Han, S. N. Murray, et al., AIP Conf. Proc. 1390 (2011) 123. [5] W. Kraus, U. Fantz, P. Franzen, et al., Rev. Sci. Instrum., 83 (2012) 02B104.
- [6] G. Serianni, P. Agostinetti, M. Agostini, et al., New J. Phys. 19 (2017) 045003 [7] B. Heinemann, U. Fantz, W. Kraus, et al., New J. Phys. 19 (2017) 015001
- [8] M. Cavenago, G. Serianni, M. De Muri, et al., Rev. Sci. Instrum. 87, 02B320 (2016). [9] V. Toigo, D. Marcuzzi, G. Serianni et al., Fusion Eng. Design 168 (2021) 112622
- [10] M. Cavenago, G. Serianni, C. Baltador, et al., AIP Conf. Proc. 2052, 040013 (2018)
- [11] E. Kralkina, P. Nekludova, A. Nikonov et al., Plasma Sources Sci. Technol. 30 (2021) 115020
- [12] D. Wunderlich, S. Mochalsky, U. Fantz, et al., Plasma S. Sci. Technol. 23 (2014) 015008 [13] M. Bacal and M. Wada, Appl. Phys. Reviews 2 (2015) 021305.
- [14] A. Hatayama, Rev. Sci. Instrum. 79 (2008) 02B901
- [15] P. N. Wainman, M. A. Lieberman, A. J. Lichtenberg et al., J. Vac. Sci. Technol. A 13 (1995) 2464
- [16] M. Barbisan IEEE Trans. Pla. Sci. (2021)
- [17] D. Pagano, C. Gorse, and M. Capitelli IEEE Trans. Pla. Sci. 35, (2007) 1247 [18] T. Mosbach, Plasma Sources Sci. Technol. 14 (2005) 610
- [19] S. H. Song, Y. Yang, P. Chabert et al., Phys. Plasmas 21, 093512 (2014)
- [20] F. F. Chen, IEEE Trans Plasma Sci 34, (2006) 718-727
- [21] M. Cavenago and S. Petrenko, 83, (2012) 02B503
- [22] V. Antoni, F. Taccogna, P. Agostinetti et al., Rendiconti Lincei Scienze Fisiche e Naturali 30 (2019) 277-285
- [23] M. Cavenago, M. Barbisan, R. Delogu, et al., Rev. Sci. Instrum. 91, (2020) 013316
- [24] M. Ugoletti, M. Agostini, M. Barbisan et al., Rev. Sci. Instrum. 92, 043302 (2021).
- [25] M. Barbisan, M. Cavenago, R. S. Delogu, et al J. Phys. Conf. Ser. (2022)
- [26] M. Cavenago and P. Veltri, Plasma Sources Sci. Technol., 23 (2014) 065024.
- [27] M. Tuszewski, Phys. Plasmas 5, 1198 (1998)
- [28] M. Cazzador, M. Cavenago, G. Serianni and P. Veltri, AIP Conf. Proc., vol. 1655, 020014 (2015).
- [29] L. C. Johnson and E. Hinnov, J. Quant. Spectrosc. Radat. Transfer. 13, (1973) 333-358
- [30] Taccogna, F., Bechu, S., Aanesland, A. et al. Eur. Phys. J. D 75 (2021), 227;
- [31] A. Shih, J. Yater, P. Pehrsson, et al., J. Appl. Phys. 82, 1860 (1997)
- [32] Y. Raitses, A. Smirnov, D. Staack, et al, Phys. Plasmas 13, 014502 (2006)
- [33] Comsol Multiphysics 3.5 (2009) or higher versions, see also <http://www.comsol.eu>
- [34] A. G. Drentje, Rev. Sci. Instrum., 74, 2631 (2003);
- [35] R. Zorat, J. Goss, D. Boilson and D. Vender, Plasma Sources Sci. Technol. 9 (2000) 161.
- [36] S. R. Walther, K. N. Leung and W. B. Kunkel, J Appl Phys 64, 3424 (1988).
- [37] P. Dhakal, Physics Open 5, 2020, 100034
- [38] N. Marconato, M. Brombin, M. Pavei et al., Fus. Eng. Design, 166, 112281 (2021) [39] M. Tuszewski, Phys. Plasmas 5, 1198 (1998)
- [40] J. T. Gudmundsson and M. A. Lieberman, Plasma Sources Sci. Technol. 6, 540 (1997)
- [41] M. A. Lieberman and A. J. Lichtenberg, Principles of Plasma Discharges and Material Processing, John Wiley, New York, 1994
- [42] G. G. Lister, Y.-M. Li, and V. A. Godyak, J. Appl. Phys., 79, 8993 (1996)
- [43] M. Cavenago, presented at Comsol2011 conference, Stuttgart.
- [44] M. Cavenago, T. Kulevoy, and S. Petrenko, Rev. Sci. Instrum., 73, 552 (2002) [
- 45] Comsol Multiphysics 3.3a, (2007), see <http://www.comsol.eu>
- [46] A. V. Phelps, J. Phys. Chem. Ref. Data, 20, 567 (1991)
- [47] M. S. Benilov, Plasma Source Sci. Technol. 18, 014005 (2009) [48] A. T. Forrester, Large Ion Beams, New York, John Wiley, 1996
- [49] I.A. Brown, The physics and Technology of Ion Sources, Wiley, 1988, 1st ed, with [11] R. Keller, 3rd chapter in ref 10, 1st ed only [12] A.T. Holmes, 4th chapter in ref 10, 1st ed only
- [50] P. T. Greenland, Proc. R. Soc. Lond. A 457, 1821 (2001)
- [51] U. Fantz et al., New Journal of Physics 8, 301 (2006)
- [52] G. Fubiani, H. P. L. de Esch, A. Simonin, R. Hemsworth, Phys. Rev. ST-AB, 11, 014202 (2008)
- [53] E. Surrey, AIP Conf. Proc. 925, 278 (2007).
- [54] J. Pamela, Plasma Phys. Control. Fusion 37 A325 1995).